

## ATOMIC SPECTROSCOPY FOR DETECTION IN THERMAL ANALYSIS\*

T. KÁNTOR, L. BEZÚR, J. SZIATISZ and E. PUNGOR

*Institute for General and Analytical Chemistry, Technical University Budapest, H-1521*

(Received June 12, 1981)

An atomic absorption spectrophotometer is coupled to a conventional thermo-analytical quartz furnace as used for TG and DTG to detect the thermally evolved products. In this combined system, the dry aerosol (smoke) obtained by cooling the vapour evolved is transported from the furnace to the flame for metal-specific atomic absorption detection. The particular design of the furnace outlet promotes the formation of stable aerosols. Optimum experimental conditions were determined, using zinc chloride solution, by varying the specimen mass, the heating rate and the flow rate of the furnace gas at a linear temperature program. The absorbance *vs.* temperature curves obtained with this method for various zinc compounds are compared with the corresponding DTG curves. The applicability of the technique for studying heterogeneous reactions with carbon tetrachloride and hexane vapours is presented. The utilization of an atomic absorption spectrophotometer equipped with a quartz cuvette for detecting the thermal evolution of mercury vapours is described, as well as detection potentials by molecular absorption (for NO and NH<sub>3</sub>) and light scattering (for smoke evolved from organic matter). The results obtained with the suggested methods may, in some respects, valuably complement the results achieved with DTG and with flame ionization detection.

The knowledge of high-temperature atomization processes is basic for developing analytical methods in optical atomic spectroscopy (OAS). The term atomization, in a wider analytical sense, involves both the volatilization of the specimen controlled by condensed-phase processes and the dissociation of the evolved species in the homogeneous gas phase. Since studies of the former processes form the main objectives of thermal analysis (TA), it is to be expected that the interrelation between OAS and TA will become closer and closer [1–3]. Intense research of the processes in question has been promoted particularly by the introduction and development of controlled-temperature electrothermal atomization (ETA) techniques discussed in comprehensive works [4, 5]. However, in ETA methods the problem frequently met with is that no separate information on condensed-phase processes is obtained. From this view, data furnished by thermoanalytical methods (TG, DTG, DTA) are useful [6], although their validity is limited owing to the differing experimental conditions. To eliminate this problem we suggested

\* Presented in part at the 24th Hungarian Conference on Analytical Spectroscopy, Miskolc, June 15–18, 1981. Abstracts pp. 159–162.

in an earlier work [7] the indirect combination of vaporization in a graphite furnace and flame atomization by introducing the dry aerosol obtained in cooling the vapour into the flame to observe atomic absorption. To produce aerosols by vaporization in graphite furnaces is one of the recent thermal dispersion methods introduced with success in *quantitative* atomic absorption and atomic emission spectrometry. In this paper one of the potential applications of this novel principle for sample introduction in thermal analysis will be discussed.

In thermal evolution analysis\* (TEA) the detection of the metals and metal compounds set free by temperature change is usually performed by mass spectroscopy (MS) [8]. In TEA-MS methods vaporization takes place at reduced pressure, the sample is transported in the form of free particles, and mass spectroscopic observation allows to study the molecular composition of the particles. The optical atomic spectroscopic detection suggested by us yields elemental, metal-specific information. Since mass losses occur in transport, the method is only suited to follow the *changes* in the rate of vaporization [7]. On the other hand, the sample is being heated in the TEA-OAS technique at atmospheric pressure and is therefore closer to the usual thermoanalytical conditions in TG, DTG and DTA. It may therefore be expected that TEA-MS and TEA-OAS techniques will do good service by complementing one another.

In our earlier paper [7] we marked two different directions for further development. One was the coupling of a quartz furnace applying the most usual thermoanalytical conditions (linear temperature program in the range of 25 to 1000°, thermocouples for temperature measurement) to an atomic absorption flame spectrophotometer (TEA-AAS). Its realization will be discussed in the present paper. The other direction consists of a graphite furnace equipped with a recording optical pyrometer (600–3000°) and coupled with a detection system similar to the above. Some preliminary results achieved in this respect have been reported recently [9]. Furnaces of certain types developed and applied originally by other authors to arc-emission [10, 11] and inductively coupled plasma [ICP] emission spectrometry can potentially be used for thermoanalytical studies too, and have already been used in part to this purpose [11]. The possible advantage of atomic emission spectroscopy (AES) for detection in thermal evolution analysis (TEA-AES) consists in the simplicity of the simultaneous study of several elements. On the other hand, the advantage of applying atomic absorption spectrophotometers consists in their applicability – with suitable supplementary devices – for molecular absorption (e.g. SO<sub>2</sub>, NO, NH<sub>3</sub>) and light-scattering studies (e.g. smoke developed from organic substances) in the 200... 800 nm wavelength

\* We consider the term Thermal Evolution Analysis (TEA) more general and as much more specific than the terms Evolved Gas Detection (EGD) and Evolved Gas Analysis (EGA) suggested earlier [8]. It is more general since it involves the detection not only of gases stable at ambient temperature, but also of aerosols, as discussed in the present paper. The term is more specific in the sense that the indication "thermal" excludes gas evolution achieved by other methods (e.g. evolution of metal hydrides from solutions).

range. Detection by molecular absorption and light scattering has been used earlier in thermal evolution analysis [8]. In the present paper we only wish to present in what manner a commercial atomic absorption instrument can be utilized for this task.

## Experimental

### Apparatus

We made use of the Du Pont Thermal Analyser Model 990 quartz furnace originally designed for TG and DTG studies, but with certain modifications (Fig. 1). In our preliminary experiments the outlet tube (inner diam. 4 mm) of the original quartz cylinder was connected to the flame. These experiments revealed that compounds vaporizing in the central part of the furnace (e.g.  $ZnCl_2$ ) partly condensed in the lower-temperature outlet tube. When increasing the temperature of the central part, the outlet tube also reached the temperature at which the condensed compound again vaporized, and resulted in a signal. This second atomic absorption signal ("memory signal") overlapped the signal corresponding to the higher sample temperature. By modifying the quartz insert as shown in Fig. 1 we were able to eliminate this problem. Here the furnace gas (containing the sample vapour too) leaving the sample space between the two necks at a flow rate of 5 . . . 20 l/h is mixed in the heated part of the quartz tube with cold carrier gas entering the tube at a flow rate of 60 . . . 240 l/h. Owing to the cooling effect of the carrier gas, the temperature of the outlet tube will not rise significantly, and hence re-evaporation will be negligible. Also, the rapid mixing of the hot sample vapour with large amounts of the cold carrier gas will presumably promote the formation of small-particle aerosol which can be transported into the flame with good efficiency (50 . . . 60%) [7]. This design also has the advantage that the temperature of the aerosol obtained by admixing the cold carrier gas does not exceed 80° even at sample space temperature of 1000°, and can therefore be transported in rubber or polyethylene tubing. The carrier gas is preferably the oxidizing gas used to pro-

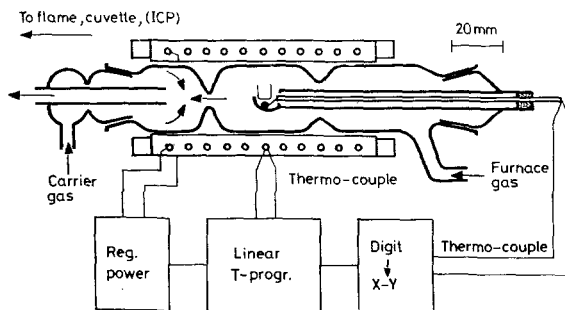


Fig. 1. Quartz furnace (modified Du Pont system) with digital temperature programmer (BME-Chinoin system)

duce the flame (air or nitrous oxide). However, inert gases (Ar, N<sub>2</sub>) can also be applied, provided that the ensuing decrease in the temperature of the flame does not largely impair the sensitivity of atomic absorption. In the present study we used air as carrier gas and an acetylene/air flame. The atmosphere in the sample space (furnace gas) can be adjusted to the requirements of the particular study. The access of the carrier gas into the sample space is prevented on the one hand by the neck formed in the quartz cylinder, and on the other hand by sucking off the aerosol (see in the followings). The furnace gases mainly used in this work were Ar, N<sub>2</sub> and CO<sub>2</sub>. For studying heterogeneous-phase halogenation the furnace gas was N<sub>2</sub> containing 8 vol. % CCl<sub>4</sub>. The device used for feeding CCl<sub>4</sub> vapour at a controlled rate has been described earlier [13]. The sample-holder cup (external diam. 4 mm, height 4 mm) is made of 0.1 mm platinum foil or of spectrally pure graphite. The cup is placed directly on the sensor head of the thermocouple whose wires are contained in a two-channel aluminium oxide ceramic holder set in a quartz tube.

The temperature programming and readout system shown in Fig. 1 has been developed in this Institute (BME) by S. Gál and co-workers [14] and is being manufactured in the Instrument-Manufacturing Department of the Pharmaceutical Works Chinoin, Budapest (Temperature Programmer Model LP 839). The signal for feedback control is produced by the thermocouple in contact with the heating wire (central part), while the thermocouple on the right-hand side measures the temperature of the sample. The instrument can provide digital readout of the temperatures valid for either chromel/alumel or Pt/Pt-Rh thermocouples, and the thermopotential can simultaneously be recorded on an X–Y recorder. In this manner, using recorder charts graduated correspondingly to the thermocouple applied, absorbance *vs.* temperature curves (AT curves) are directly obtained. In the halogenating atmosphere the use of Pt/Pt-Rh thermocouple was necessary, but all other measurements were performed with chromel/alumel thermocouple. The linearity and reproducibility of the temperature program were found satisfactory (see Fig. 4 in the following section). At a heating rate set to the nominal value of 50°/min, e.g., the factual values measured at 200, 500 and 900° were 49.5°/min, 56°/min and 52°/min.

In Fig. 1 we have marked the possibility to transport the aerosol into an inductively coupled plasma (ICP) for emission spectrometric detection [12]. This subject will not, however, be dealt with in this paper.

A Pye Unicam Model SP 90A atomic absorption spectrophotometer was used to detect the products evolved in the furnace. The part for introducing the sample was, however, modified (Fig. 2). The concentric nebulizer serving for pneumatic spraying of the sample solutions and its gas-introducing part were removed and replaced by the gas injector shown in Fig. 2, which simultaneously allowed the introduction of the oxidizing gas. The injector was made in our own workshop. The internal diameter of the metal capillary in the gas injector is 0.6 mm. By passing the oxidizing gas having a pressure of about 2 bar through the capillary, a sufficient sucking effect is obtained in the tube end pointing upwards, which is

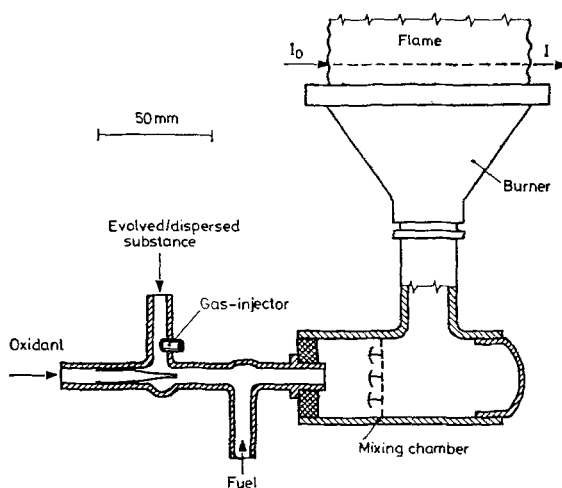


Fig. 2. Gas injector, mixing chamber and burner system for flame atomic absorption measurements

connected by a length of about 20 cm polyethylene tubing to the outlet tube of the furnace (Fig. 1).

In the present studies we used a stoichiometric acetylene/air flame (mixing ratio 0.125) by setting the following flow rates (1 bar): acetylene 1.0 l/min; air through the capillary (injector gas 5.0 l/min; aerosol-transporting air (carrier gas) 3.0 l/min. The observation height of the flame was set to 10 mm. the flow rates of acetylene and injector gas were adjusted by using the needle valves and flow gauges belonging to the Pye instrument, that of the carrier gas by means of a screw installed in the injector (Fig. 2) and a separate flow gauge. In the simplest mode of operation the inlet port for the carrier gas in the furnace part of the apparatus (Fig. 1) is left open, and thus the carrier gas is obtained from the surrounding air. It should be noted that the above (or a mainly similar) modification can be carried out in a simple way with practically all commercial atomic absorption spectrophotometers, but the types with relatively low-volume mixing chambers and burner heads ( $<300 \text{ cm}^3$ ) should be preferred to provide short transport time of the aerosol ( $<2 \text{ s}$ ) considering the total gas flow rate [7]. Atomic absorption spectrophotometers can usually be also operated in the flame emission mode, eminently suitable, e.g. for atomic emission detection of alkali metals and molecular emission detection of sulphur and phosphorus [15, 16].

In Fig. 3, two types of quartz flow cuvettes now in common use for atomic absorption spectrometry measurements are shown: above, a type to detect mercury vapours evolved from solutions, below, a type to detect metal hydrides [17]. The latter type is heated with an acetylene/air flame or with an electric heating element to decompose the hydrides. In our present studies we applied the "cold" cuvette for detecting the mercury vapour evolved in the furnace by atomic absorption spectroscopy (AAS) and NO and  $\text{NH}_3$  gases by molecular absorption spectroscopy

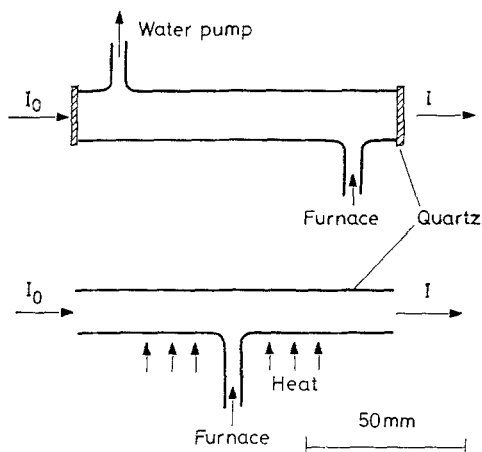


Fig. 3. Quartz cuvettes adjustable to the burner head. Above: cold cuvette, below: heatable cuvette

copy (MAS), as well as for detecting the smoke evolved by heating from organic substances by light scattering. Up to the present we only used the heatable cuvette in some preliminary studies. The primary radiation sources were suitable hollow cathode lamps for AAS and deuterium lamp for MAS and light scattering measurements.

For comparison, TG and DTG measurements were performed for the zinc compounds, using a Du Pont Thermal Analyser Model 990, and for organic substances, thermal evolution measurements using the Du Pont Thermal Evolution Analyser Model 916 operating with a flame ionization detector.

## Results

In the followings we wish to present the experimental results obtained with TEA-AAS, as well as with the related TEA-MAS and light scattering methods, and — in part — compare these results with those obtained by DTG and TEA now in general use. A detailed analysis of the experimental data would exceed the frame of this paper.

### *Studies of zinc compounds (AAS)*

For TEA-AAS measurements, the zinc compounds were introduced into the furnace either in the form of solutions or in the solid form. The comparative DTG measurements were performed with solid specimens.

*Zinc chloride.* 7% water is liberated from the analytical-grade zinc chloride used in our experiments when heated to 100°. Methanolic solutions prepared of this substance were utilized to determine optimum experimental conditions by varying

the mass of specimen, the heating rate and the flow rate of the furnace gas (Figs 4, 5 and 6). Identical volumes ( $2 \mu\text{l}$ ) of the solutions were pipetted into the platinum cup. In all experiments (also in the followings) the cup was cleaned after each heating-up ( $450 \dots 500^\circ$ ) by boiling in HCl diluted 1 : 1 and subsequent ignition in a flame. This procedure was necessary, because zinc chloride partly underwent hydrolysis in the not completely anhydrous solutions, and zinc oxide residue was left over in the cup (see in the followings). In all experiments two replicates were made. The slot of the burner head was adjusted perpendicularly to the light path, in order to reduce the sensitivity of atomic absorption measurement.

As demonstrated by Figs 4 and 5, the increase of both specimen mass and heating rate shifts the maximum of the vaporization rate towards higher temperatures, similarly as in DTG [8]. The same applies to the final temperature of vaporization, whereas the initial temperature of vaporization appeared practically constant ( $300^\circ$ ) and independent of the above parameters. This temperature can hence be considered as the temperature characterizing the substance being tested [7]. According to Fig. 6 the initial temperature of vaporization remained unchanged in the  $10 \dots 20 \text{ l/h}$  flow rate range of the furnace gas, but the A-T curve was shifted towards lower temperatures by  $25^\circ$  at a flow rate of  $30 \text{ l/h}$ . We selected  $20 \text{ l/h}$  as the optimum value for further experiments.

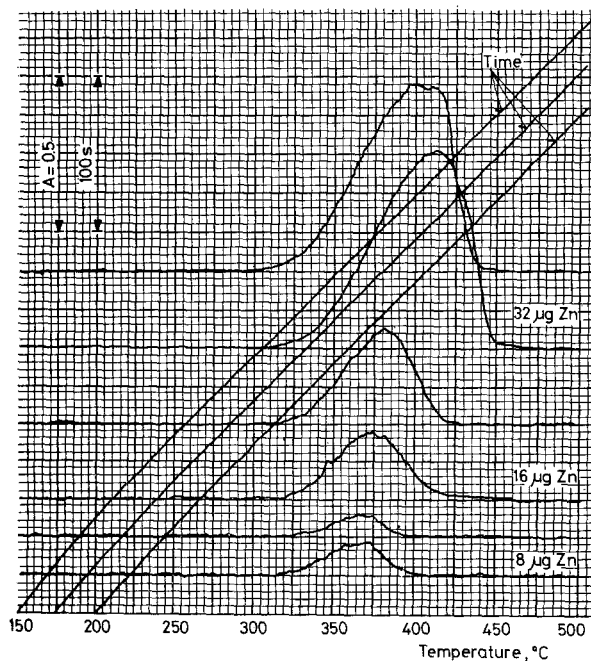


Fig. 4. A-T curves of methanolic zinc chloride solutions with varying specimen masses (8, 16,  $32 \mu\text{g Zn}$ ). Platinum cup, heating rate  $50^\circ/\text{min}$ , furnace gas  $20 \text{ l/h N}_2$ , flame AAS at the  $213.9 \text{ nm}$  zinc line. The heating time *vs.* temperature curves are shifted stepwise along the ordinate

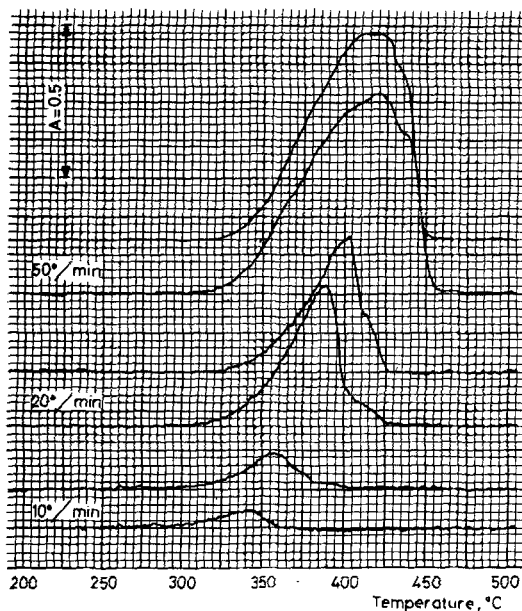


Fig. 5. A-T curves of a methanolic zinc chloride solution ( $32 \mu\text{g Zn}$ ) with variable heating rate (10, 20,  $50^\circ/\text{min}$ ). Other conditions identical to those indicated in Fig. 4

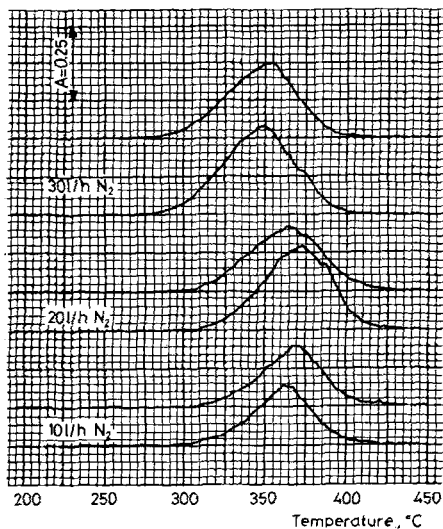


Fig. 6. A-T curves of a methanolic zinc chloride solution ( $16 \mu\text{g Zn}$ ) with variable furnace gas flow rate (10, 20, 30 l/h). Other conditions identical to those indicated in Fig. 4.



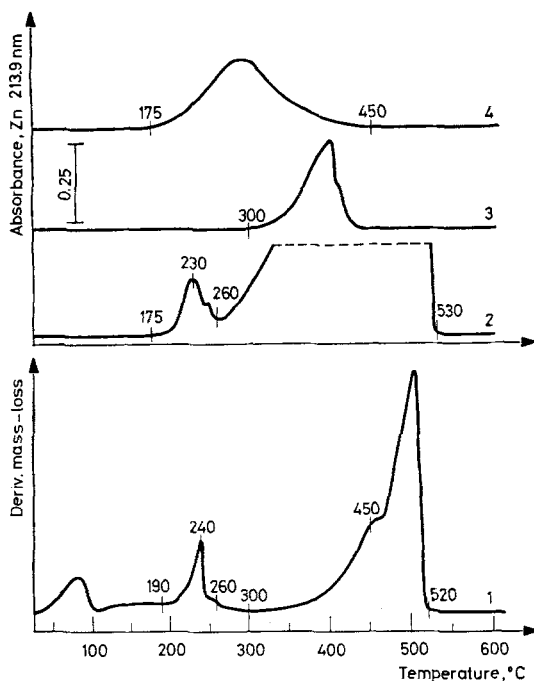


Fig. 7. DTG curves (below) and AT curves (above) of zinc chloride. 1 — 7 mg solid sample; 2 — 1 mg solid sample; 3 — methanolic solution, 0.08 mg  $ZnCl_2$ ; 4 — zinc oxide residue after addition of hydrochloric acid

In Fig. 7 the results of derivative thermogravimetry (DTG) (below) and TEA-AAS (above) are compared. The values presumably marking identical transformations (initial, peak, inflexion and final temperatures) are indicated on both DTG and A-T curves. On the DTG curve (1) the gas evolved up to 100° (7%) is adhering water. The product evolved in the 190...260° range could assumably be either hydrochloric acid produced by hydrolysis or partially combined water. According to the A-T curve 2 also obtained with solid zinc chloride this transformation, however, is related to the evolution of some sort of zinc compound. The second initial temperature on the DTG curve, 300°, corresponds to the initial temperature of the A-T curve 3 obtained with a methanolic zinc chloride solution specimen. The A-T curve 4 was obtained by pipetting 5  $\mu$ l of concentrated hydrochloric acid into the cup after the previous measurement (which gave curve 3) and heating without intermediate drying. The zinc oxide residue left in the platinum cup after the previous heating gave a zinc compound with the hydrochloric acid, a compound starting to vaporize at 175° and presumably identical with the compound evolved from solid zinc chloride in the 190...260° temperature range (curves 1 and 2).

*Zinc ammonium chloride.* We prepared aqueous solutions corresponding to the formula  $ZnCl_2 \cdot 2 NH_4Cl$  from zinc chloride and ammonium chloride. The A-T

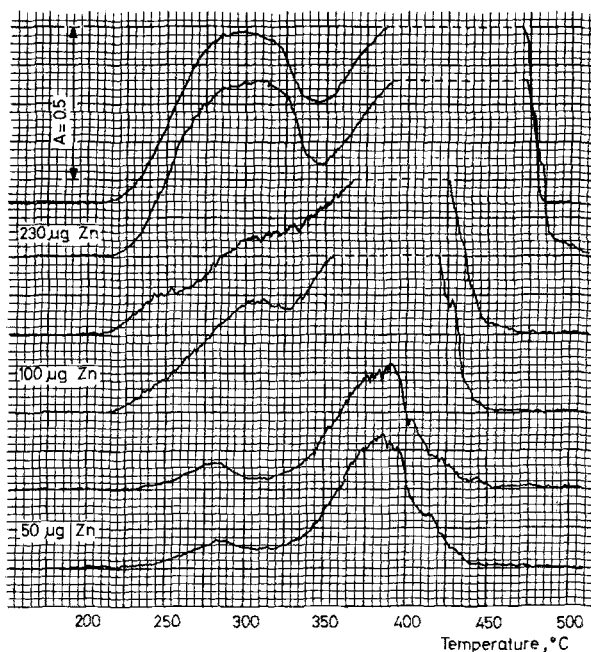


Fig. 8. A-T curves of aqueous zinc ammonium chloride solutions with variable specimen mass (50, 100, 230  $\mu\text{g}$  Zn). Platinum cup, heating rate  $20^\circ/\text{min}$ , furnace gas 20 l/h  $\text{N}_2$ , flame AAS. 213.9 nm zinc line

curves obtained with increasing specimen masses are presented in Fig. 8. The curves have two maxima, the first initial temperature being at  $200^\circ$  (this can be read more exactly at higher specimen masses), and a second initial temperature around  $300^\circ$  at low specimen masses. The latter temperature is also a preferential point in the experiments performed with zinc chloride (cf. Fig. 7).

Figure 9 presents the DTG curves 1, 2, 3 obtained with solid specimens (below) and the A-T curves 4 and 5 obtained with solutions (above). The solid  $\text{ZnCl}_2 \cdot 2\text{NH}_4\text{Cl}$  specimen was made by evaporation to dryness of a solution having the corresponding composition and subsequent drying of the product. DTG measurements were also performed with solid  $\text{NH}_4\text{Cl}$  and with solid zinc ammonium chloride containing 34% excess  $\text{NH}_4\text{Cl}$ . As demonstrated by curves 1 and 2, the initial sublimation temperature of free  $\text{NH}_4\text{Cl}$  is  $150^\circ$ , while the initial temperature in the DTG curve 3 corresponding to stoichiometric  $\text{ZnCl}_2 \cdot 2\text{NH}_4\text{Cl}$  is  $200^\circ$ , identical with the initial temperatures of the according A-T curves 4 and 5. Consequently the first DTG peak originates from the evolution of a zinc compound. This statement could not have before been made unambiguously.

In our earlier studies performed with the combination of a graphite furnace and flame spectrophotometer [7], the heating rate below  $400^\circ$  was around  $600^\circ/\text{min}$ , and the specimen mass was in the order of 100 ng. The initial temperatures of the

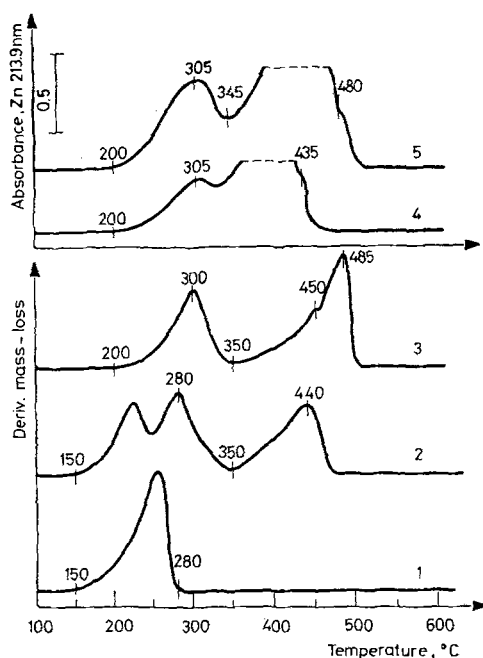


Fig. 9. DTG curves (below) and A-T curves (above) of ammonium chloride and zinc ammonium chloride. 1 - 3 mg solid  $\text{NH}_4\text{Cl}$ ; 2 - 4.3 solid  $\text{ZnCl}_2 \cdot 2 \text{NH}_4\text{Cl}$  + 2.2 mg solid  $\text{NH}_4\text{Cl}$ ; 3 - 6.8 mg solid  $\text{ZnCl}_2 \cdot 2 \text{NH}_4\text{Cl}$ ; 4 - 0.37 mg  $\text{ZnCl}_2 \cdot 2 \text{NH}_4\text{Cl}$  in methanolic solution; 5 - 0.85 mg  $\text{ZnCl}_2 \cdot 2 \text{NH}_4\text{Cl}$  in methanolic solution

A-T curves for zinc chloride and zinc ammonium chloride solutions were higher than in the present studies, and the shape of the curves also significantly differed from those presented in this paper. We consider the temperature measurement achieved with the present system as the more accurate.

#### *Heterogeneous reactions with $\text{CCl}_4$ and $\text{C}_6\text{H}_{14}$ vapours (AAS)*

In modelling metallurgical processes applying gaseous halogenating agents, isothermal studies are usually performed as for instance, in a recent study on isothermal chlorination kinetics of  $\gamma\text{-Al}_2\text{O}_3$  utilizing carbon tetrachloride vapour [18]. Presumably, however, a study of heterogeneous halogenation according to a dynamic temperature program might also be of interest. The TEA-OAS technique offers ready potentials for this purpose. Recently we investigated the spectrophotometric utilization of heterogeneous halogenation in our laboratory, making use of a graphite furnace [9] and arc discharge between graphite electrodes [13]. In the present work with zinc nitrate solutions we also studied the reactivity of hexane ( $\text{C}_6\text{H}_{14}$ ) vapour. In the measurements we used both platinum and graphite cups. The furnace gas was nitrogen containing 8 vol.%  $\text{CCl}_4$  and 12 vol.%  $\text{C}_6\text{H}_{14}$  vapour, resp. [13].

According to our earlier experiments with aqueous zinc nitrate solution in platinum cups [7] the A-T curve starts at 1300°, corresponding to the initial temperature of zinc oxide sublimation. When using a graphite cup, the initial temperature of vaporization is 850 . . . 870°, characterizing the temperature of the reaction  $\text{ZnO}_{(s)} + \text{C}_{(s)} = \text{CO}_{(g)} + \text{Zn}_{(g)}$ . The A-T curves for zinc nitrate solution in the presence of  $\text{CCl}_4$  and  $\text{C}_6\text{H}_{14}$  vapours in both cups are presented in Fig. 10, demonstrating that on the porous graphite surface the initial temperature of the reaction is lower in the case of both agents than on the platinum surface. On the other hand, on the platinum surface the reaction takes place in a narrower temperature range. The initial temperatures obtained with  $\text{CCl}_4$  (290° in the graphite cup and 360° in the platinum cup) presumably correspond to the reaction  $2 \text{ZnO} + \text{CCl}_4 = 2 \text{ZnCl}_2 + \text{CO}_2$  [19], since formation of free gaseous  $\text{Cl}_2$  from  $\text{CCl}_4$  starts at about 500° only [18].

Indirect combinations of quartz furnaces with flame spectrophotometry can be utilized for quantitative analytical purposes, as demonstrated by the analytical curves shown in Fig. 11. The values on the ordinate axis are time-integrated absorbance values for zinc, copper and lead measured at the resonance lines indicated in the figure, using suitable hollow cathode lamps. For integrating, the Electronic Integrator manufactured by MOM, Budapest was used. In the cases of copper and lead the slot burner head was in the normal position (cf. Fig. 2), for zinc it was

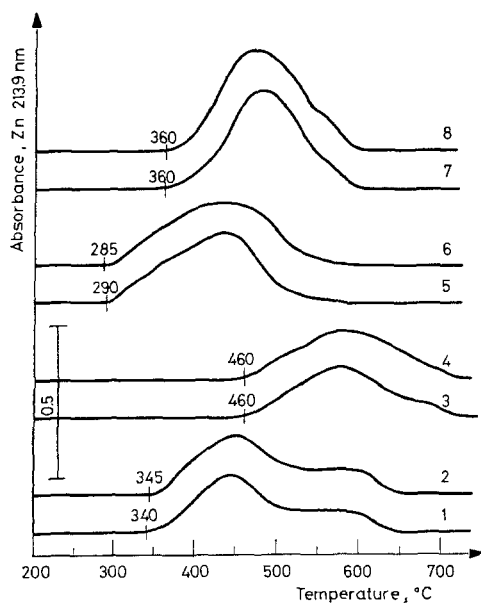


Fig. 10. A-T curves of aqueous zinc nitrate solution ( $10 \mu\text{g Zn}$ ) heated in  $\text{N}_2$  containing carbon tetrachloride and hexane vapours, resp. 1 and 2 — hexane, graphite cup; 3 and 4 — hexane, platinum cup; 5 and 6 —  $\text{CCl}_4$ , graphite cup; 7 and 8 —  $\text{CCl}_4$ , platinum cup

adjusted perpendicularly to the light path. Nitrogen furnace gas of 30 l/h flow rate, containing 8 vol. %  $\text{CCl}_4$  vapour was used. The carrier gas was air at a flow rate of 240 l/h. Increasing amounts of the metal nitrate solutions (5...20  $\mu\text{l}$ ), separately for each metal, were pipetted into graphite cups. The furnace was pre-heated to  $750^\circ$ , so that, in the case of rapid specimen insertion, a heating rate of  $1100 \dots 800^\circ/\text{min}$  could be attained in the  $150 \dots 500^\circ$  temperature range (cf. Fig. 12). The cup containing the solution was first moved into the mouth part of the furnace and evaporation to dryness was followed on the basis of the temperature change (digital readout). When the temperature of the cup reached  $120^\circ$ , the holder rod was completely pushed in, moving the cup into the centre of the furnace. The atomic absorption signal was integrated for 10 seconds. During this period all three metal compounds totally vaporized in the chlorinating atmosphere.

The results summarized in Fig. 11 confirm our earlier finding [7] that the mass of the substance entering the flame is proportional to the mass of the vaporized substance. Studies performed with various substances indicated that the value of the proportionality factor is 0.5...0.6. These studies, however, also indicated a dramatic decrease of this value above a defined rate of vaporization, this being equivalent to inferior transport efficiency of the aerosol. By correctly selecting the specimen mass and the heating rate, the vaporization rate can be kept below this critical value.

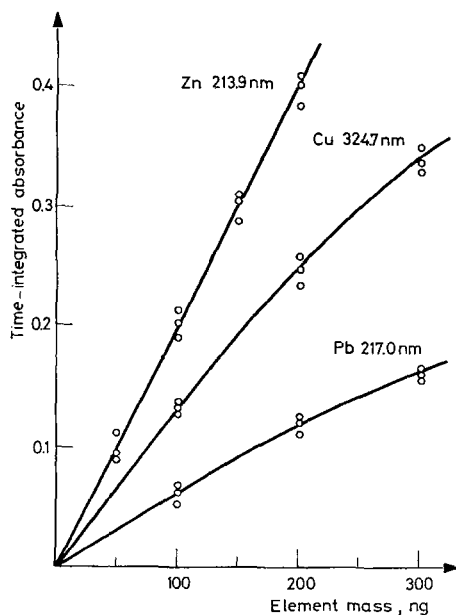


Fig. 11. Atomic absorption analytical curves of zinc, copper and lead in dilute nitric acid solutions using halogenating atmospheres

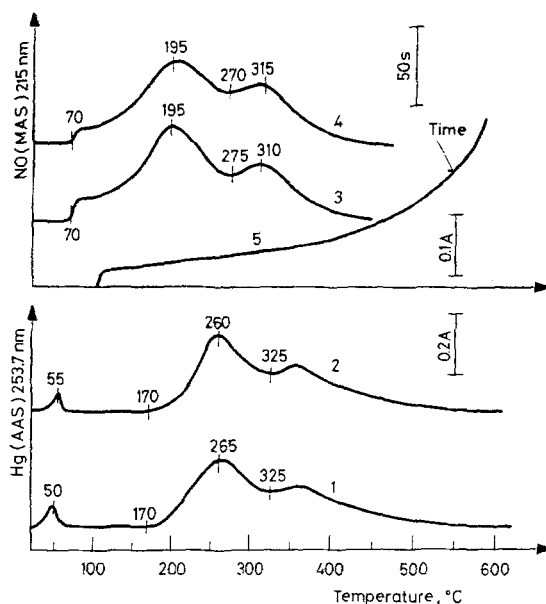


Fig. 12. Atomic Absorption A-T curves of aqueous mercury nitrate solution (below) and NO molecular absorption AT curves of aqueous mercury nitrate solution (above). Quartz cuvettes. 1 and 2 —  $1.6 \mu\text{g Hg}(\text{NO}_3)_2$ , heating rate  $50^\circ/\text{min}$ ; 3 and 4 —  $32 \mu\text{g Hg}(\text{NO}_3)_2$ , heating program as indicated in curve 5

### *Studies of mercury nitrate by AAS and MAS*

The aqueous solution of mercury nitrate was measured in a graphite cup, using  $\text{CO}_2$  furnace gas at a flow rate of 20 l/h. The products were swept into a cuvette with quartz windows (Fig. 3, above) with carrier air at a flow rate of 60 l/h.

The A-T curves of the thermally evolved mercury vapour are presented in the lower part of Fig. 12 (mercury hollow cathode lamp, 253.7 nm wavelength) for a heating rate of  $50^\circ/\text{min}$ . The curves indicate that a small amount of mercury is evolved from the aqueous solution already in the range of  $30 \dots 70^\circ$ . In the case of (1 + 1) nitric acid solutions this first peak did not appear. From dry mercury nitrate the evolution of mercury vapour starts at  $170^\circ$  and proceeds in two stages.

To detect the NO molecule evolved from the mercury nitrate solution at the wavelength 215 nm [20] we used a deuterium lamp (Fig. 12, above). For the purpose of these molecular absorption spectrometric measurements we increased the concentration of mercury nitrate by a factor of 20 and preheated the furnace to  $600^\circ$ . When the specimen reached the temperature of  $100^\circ$  in the mouth part of the furnace (drying), the sample holder was inserted totally into the furnace. In this manner we achieved the time *vs.* temperature curve 5. According to this program the temperature increase is close to linear and the heating rate is  $1030^\circ/\text{min}$

in the 120 . . . 350° range. Curves 3 and 4 indicate that the evolution of NO starts at 70° from the aqueous solution, and after drying, two further peaks are observed, similarly to the evolution of mercury vapour (curves 1 and 2). In the range above 100°, the appearance of mercury vapour approximately coincides with the maximum rate of NO formation. It may also be seen that NO evolution largely overlaps with the evolution of mercury vapour.

We wish to mention that the polyethylene tube connecting the furnace and the cuvette became significantly soiled with mercury deposits originating from the mercury vapours evolved in NO measurements, where relatively large amounts of mercury nitrate were applied. The interfering effect of these deposits showed up when – after NO measurements – we returned to the detection of mercury vapour by atomic absorption. In such cases it is necessary to change the polyethylene tube and clean the cuvette by passing a suitable amount of gas through it. We also wish to note that the determination of  $\text{NH}_3$ ,  $\text{SO}_2$ ,  $\text{H}_2\text{S}$ ,  $\text{NO}_2$  molecules by gas-phase molecular absorption spectrometry, has also been reported in the literature [21–23]. Presumably the thermoanalytical utilization of these measurements by means of the present measuring system might also be of interest.

### Studies of organic substances

Molecular gases formed in the thermal decomposition of organic substances can be studied by MAS detection, and the smoke (aggregated solid particles) formed by light scattering detection. We suggest the terms TEA-MAS and TEA-RSD (Radiation Scattering Detection) for these methods. It should, however, be underlined that the differentiation between intensity decreases due to molecular absorption and light scattering, resp., will generally require special studies (see in the followings).

*Ammonium pyrrolidine dithiocarbamate.* We assumed that the thermal decomposition of APDC yields  $\text{NH}_3$  gas whose absorption can be measured at 201 nm [20, 22]. The experimental conditions applied were: 5 mg specimen mass, graphite cup, 20 l/h  $\text{N}_2$  furnace gas, 60 l/h carrier air, 50°/min heating rate. The A-T curves are presented in the upper part of Fig. 13, indicating the initial temperature of  $\text{NH}_3$  evolution at 50°, and a second protracted peak starting at 135 . . . 140°. The final temperature of the decomposition is around 300°, taking into account the shift of the base line due to the soiling of the quartz cuvette window as a result of the large specimen mass. The shift can be eliminated by using the open cuvette type shown in the lower part of Fig. 3. This was found in later studies, which, however, will not be dealt with here.

The lower part of Fig. 13 shows the TEA-FID curve obtained with flame ionization detection. Conditions were 32°/min heating rate (the maximum that could be achieved with the apparatus in this experiment), 1.8 l/h  $\text{N}_2$  furnace gas, 5 mg specimen mass, graphite cup. The very large specimen mass was chosen to obtain

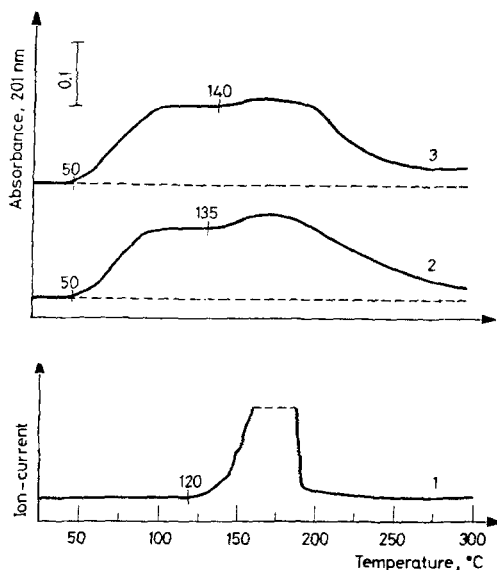


Fig. 13. Thermal evolution curves of ammonium pyrrolidine dithiocarbamate detected by flame ionization (below) and by  $\text{NH}_3$  molecular absorption (above). 5 mg solid specimen

data comparable with those of TEA-MAS (for the TEA-FID method, specimen masses less by several orders of magnitude would have been sufficient). As known, the TEA-FID technique records the evolution of carbon-containing compounds only. According to curve 1, their evolution starts at  $120^\circ$ , reaches the maximum rates at about  $175^\circ$  and ends at  $220^\circ$ .

It may be assumed that the second peak in the A-T curves with the initial temperature of  $135 \dots 140^\circ$  corresponds to the light scattering originated from the smoke detected with the FID method. However, the A-T curves indicate, in addition, the evolution of  $\text{NH}_3$  and of smoke consisting of non-carbon-containing particles which takes place in a much larger temperature range. Hence, the present MAS and RDS signals overlap. Their separation might, on principle, be performed on the basis that the RSD signal is observable in a broader wavelength range. Presumably a separate observation of the smoke signal will appear possible at some non-molecular-specific wavelength in the vicinity of the  $\text{NH}_3$  band. We intend to study this problem in our future work.

*Cellulose and cellulose nitrate.* The conditions were similar to those applied in the experiments with APDC, with the difference that specimen mass was 1 mg and optical measurements were performed at 250 nm. With cellulose and cellulose nitrate no molecular absorption appears at this wavelength, so that the A-T curves (Fig. 14, above) correspond to pure TEA-RSD measurements. The corresponding TEA-FID curves are presented in the lower part of Fig. 14.



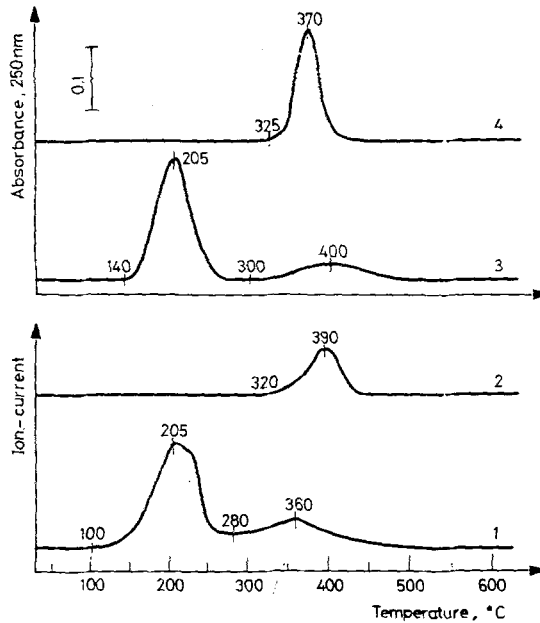


Fig. 14. Thermal evolution curves of cellulose and cellulose nitrate detected by flame ionization (below) and by light scattering (above). 1 mg solid specimen. 1 and 3 — cellulose nitrate; 2 and 4 — cellulose

It can be observed that the preferential points of curve 1 and curve 3 referring to cellulose nitrate and obtained by TEA-FID and TEA-RSD, resp., agree within 40°. The agreement is even better between the corresponding curves 2 and 4 referring to cellulose. It should be remembered in the context of this comparison that the FID method senses not only organic aggregates, but carbon-containing free molecules and radicals too. Also, in the FID technique the time at disposal for aggregate formation (the transport path length) is shorter.

Up to the present we have not studied the dependence of the TEA-RSD curves on wavelength in detail. It is known that the intensity of light scattering depends on the degree of dispersion of the aerosol and on the wavelength of the illuminating radiation source. This question is dealt with also in the literature for atomic absorption [17, 24]. If the diameter of the particles exceeds the wavelength, the intensity of the scattered light only slightly depends on wavelength (MIE scattering). If, however, particle diameter is essentially below the wavelength, the intensity of the scattered light is inversely proportional to the fourth power of the wavelength (Rayleigh scattering). Experiences indicated that it is rather the latter relationship which prevails in atomic absorption measurements [17]. Should the Rayleigh-relationship be valid for the present TEA-RSD method too, sensitivity can be increased largely by using shorter wavelength radiation for illumination.

\*

The authors wish to express their thanks to S. Gál for his assistance in the present application of the temperature programmer developed by him and his group, and for the valuable discussions on the subject. Thanks are also due to K. Tomor and J. Kőmives who participated in the comparative thermoanalytical measurements and their analysis.

### References

1. WILSON and WILSON's Comprehensive Analytical Chemistry (Ed. G. Svehla), T. Kántor, Emission Spectroscopy, Elsevier, Amsterdam, 1975 Vol. V, pp. 65–69.
2. S. GÁL and T. KÁNTOR, *Periodica Polytech.*, (Chem. Eng.), 18 (1974) 9.
3. T. KÁNTOR and E. PUNGOR, *J. Thermal Anal.*, 6 (1974) 521.
4. B. V. L'VOV, *Atomic Absorption Spectrochemical Analysis*, Elsevier, New York, 1970.
5. C. W. FULLER, *Electrothermal Atomization for Atomic Absorption Spectrometry*, The Chemical Society, London, 1977.
6. R. E. STURGEON, C. L. CHAKRABARTI and C. H. LANGFORD, *Anal. Chem.*, 48 (1979) 357.
7. T. KÁNTOR, E. PUNGOR, J. SZTATISZ and L. BEZUR, *Talanta*, 26 (1979) 357.
8. W. W. WENDLANDT, *Thermal Methods of Analysis*, 2nd ed., Wiley, New York, 1974.
9. T. KÁNTOR and E. PUNGOR, 6th Polish Conference on Analytical Spectroscopy, Bielo-wieża, Poland 1981, Abstracts pp. 12–13.
10. E. GEGUS, J. KREITER, L. MÉRAY and J. INCZÉDY, *Acta Chim. Acad. Sci. Hung.*, 100 (1979) 221.
11. E. GEGUS, J. KREITER, L. MÉRAY and J. INCZÉDY, *Acta Chim. Acad. Sci. Hung.*, 101 (1979) 347.
12. A. M. GUNN, D. L. MILLARD and G. F. KIRKBRIGHT, *Analyst*, 103 (1978) 1066.
13. T. KÁNTOR, É. HANÁK-JUHAI and E. PUNGOR, *Spectrochim. Acta*, 358 (1980) 401.
14. Hung. Patent No. 173431/1977.
15. C. VEILLON and J. Y. PARK, *Anal. Chim. Acta*, 60 (1972) 293.
16. G. L. EVERETT, T. S. WEST and R. W. WILLIAMS, *Anal. Chim. Acta*, 68 (1974) 387.
17. W. J. PRICE, *Spectrochemical Analysis by Atomic Absorption*, Heyden, London, 1979.
18. I. BERTÓTI, I. S. PAP, T. SZÉKELY and A. TÓTH, *Thermochim. Acta*, 41 (1980) 27.
19. I. NÁRAY-SZABÓ, *Inorganic Chemistry (in Hungarian)*, Akadémiai Kiadó, Budapest, 1956, Vol. I, p. 501.
20. R. W. B. PEARSE and A. G. GAYDON, *The Identification of Molecular Spectra*, Wiley, New York, 1950.
21. M. S. CRESSER and P. J. ISAACSON, *Talanta*, 23 (1976) 885.
22. M. S. CRESSER, *Anal. Chim. Acta*, 85 (1976) 253.
23. M. S. CRESSER, *European Spectroscopy News*, 19 (1978) 36.
24. S. R. KOIRTYOHANN and F. E. PICKETT, *Anal. Chem.*, 38 (1966) 1087.

ZUSAMMENFASSUNG — Ein Atomabsorptionsspektrometer wurde mit einem konventionellen thermoanalytischen Quarzofen gekoppelt um thermische Abspaltprodukte nachzuweisen. In diesem kombinierten System wird das durch Kühlung des entwickelten Dampfes erhaltene Aerosol (Rauch) vom Ofen in die Flamme für den metallspezifischen Atomabsorptionsnachweis übergeleitet. Die spezielle Ausbildung der Austrittsöffnung gewährleistet die Bildung eines stabilen Aerosols. Die optimalen Versuchsbedingungen wurden durch Zinkchloridlösungen bei Änderung der Probenmasse, der Aufheizgeschwindigkeit und der Strömungsgeschwindigkeit des Ofengases im linearen Temperaturprogramm ermittelt. Die mit dieser Methode für verschiedene Zinkverbindungen erhaltenen Absorptions-Temperatur-Kurven wurden mit den entsprechenden DTG-Kurven verglichen. Die Anwendbarkeit dieser Technik bei dem Studium heterogener Reaktionen mit Kohlenstofftetrachlorid und Hexandämpfen wird gezeigt. Der Einsatz eines mit einer Quarzküvette zum Nachweis der thermischen Ent-

wicklung von Quecksilberdampf versehenen Atomabsorptionsspektrometers wird beschrieben, sowie die Nachweisgrenze durch molekulare Absorption (für NO und NH<sub>3</sub>) und Lichtstreuung (für aus organischem Material entwickelten Rauch). Die bei den beschriebenen Methoden erhaltenen Ergebnisse können, in mancher Hinsicht, die durch DTG und Flammenionisationsnachweis erhaltenen Ergebnisse wertvoll ergänzen.

Резюме — Атомно-абсорбционный спектрофотометр был соединен с обычной термоаналитической кварцевой печью, используемой в ТГ и ДТГ для обнаружения веществ, выделяющихся при термическом процессе. В такой комбинированной системе сухой аэрозоль (дым), полученный охлаждением выделенного пара, переносится из печи в пламя для регистрации специфичного атомного поглощения металлом. Особая конструкция выпускного отверстия печи способствует образованию стабильного аэрозоля. На примере растворов хлористого цинка установлены оптимальные экспериментальные условия путем изменения массы частиц, скорости нагрева и скорости потока газа печи при линейном программировании температуры. Графики в координатах поглощение — температура, полученные этим методом для различных соединений цинка, сопоставлены с соответствующими ДТГ-кривыми. Показано применение этого метода для изучения гетерогенных реакций с четыреххлористым углеродом и парами гексана. Описано использование атомно-абсорбционного спектрофотометра, снабженного кварцевой кюветтой, для обнаружения термически выделенных паров ртути, наряду с потенциалами регистрации с помощью молекулярного поглощения (для NO и NH<sub>3</sub>) и рассеяния света (для дыма, выделяющегося из органического вещества). Результаты, полученные предложенными методами, могут в известной мере служить ценным дополнением к результатам, полученными с помощью ДТГ и пламенно-ионизационной регистрации.